Desalination and Water Treatment
www.deswater.com

doi: 10.5004/dwt.2020.26131

200 (2020) 296–303
October

Adsorption properties of reactive dyes on the activated carbon from corn straw prepared by microwave pyrolysis

Xiaoli Ren[a,*], Shangwen Wang[a], Yuqiang Jin[b], Defei Xu[b], Hongbing Yin[b]

[a]*Department of Environment and Safety Engineering, Taiyuan Institute of Technology, Yingxin Street 030008, Taiyuan City, Shanxi Province, PR China, emails: xlren66@126.com (X. Ren), 972382224@qq.com (S. Wang)*
[b]*First Branch Factory, Shanxi North Xing'an Chemical Industry Co., Ltd., Xinlan Road 030008, Taiyuan City, Shanxi Province, PR China, emails: jyq91@126.com (Y. Jin), xvdefei@163.com (D. Xu), 79598747@qq.com (H. Yin)*

Received 13 September 2019; Accepted 18 May 2020

ABSTRACT

A low cost activated carbon from corn straw was prepared by dry pyrolysis using the microwave, the S_{BET} of activated carbon was 937 m^2 g^{-1}. The adsorption of Reactive Brilliant Yellow K-6G and Reactive Brilliant Red K-2BP on the activated carbon from corn straw were investigated. Four types of kinetic models and three types of isotherms were used to fit the experimental data. The results showed that the adsorption of RBY K-6G and RBR K-2BP on the activated carbon from corn straw both followed the pseudo-second-order kinetic model and Langmuir isotherm. The enthalpy change ($\Delta H°$) and Gibbs free energy ($\Delta G°$) are calculated, $\Delta H° > 0$ and $\Delta G° < 0$ suggested that the adsorption process was endothermic and spontaneous in nature.

Keywords: Adsorption; Reactive dye; Corn straw; Activated carbon; Microwave

1. Introduction

Dyes and pigments are generally used in textile, paper production, food technology, and so on. The discharges of dye effluent into the environment are considered as harmful to aquatic life and public health [1]. Therefore, various treatment methods were studied to remove dyes from aqueous solutions, including electrocoagulation [2,3], photocatalysis [4,5], coagulation [6], biodegradation [7,8], adsorption [9], membrane treatments [10], and so on. Among them, adsorption process aroused people's wide concern, and various low–cost adsorbents have been prepared to remove dyes from their solutions [11]. Sohrabi and Ameri [1] used sesame hull waste as an adsorbent to adsorb Reactive Brilliant Red 141 in a batch process. Qiu et al. [12] prepared the activated carbon from capsicum straw to remove Methylene Blue. Honório et al. [13] used soybean hulls as the adsorbent, studied the adsorption properties of reactive blue BF-5G. Ratnamala et al. [14] used sawdust from Malaysian teak wood to adsorb reactive blue dye. In addition, other researchers have also developed different adsorbents to remove reactive dyes, such as RB 5, RBR X-3B, RLY K-6G, RBB X-BR, RBR 2, RBY 145A, RBR 195A, and so on [15–18].

In this work, corn straw was used to prepare the activated carbon. In the carbonization process, microwave heating replaced traditional heating. Microwave heating does not need to heat the material directly from outside to inside when compared to conventional heating, but rather through the energy dissipation of the microwave inside the material. Depending on the nature of the material (conductivity, permeability, and dielectric constant), the microwave can directly and efficiently generate heat throughout the material. As a result, the carbonation time in this study was only 6 min at the power of 700 W. However, in traditional heating, it usually takes 60 min at about 400°C or higher

* Corresponding author.

temperature. In addition, we have simplified the preparation steps of chemical activation method. As we all know, in the preparation process of activated carbon using traditional chemical activation method, the materials usually need to be immersed in the activator solution for a period of time, then dehydrated and pyrolyzed, some need to be dried before pyrolysis. The traditional method will result in activator residue in the impregnation solution and more energy consumption. In this experiment, the steps of impregnation and dehydration were omitted. Zinc chloride solution and corn straw were mixed thoroughly in half-dry or half-wet state, and then pyrolyzed to obtain the activated carbon. The adsorption kinetics, isotherm, and thermodynamics of Reactive Brilliant Yellow K-6G (RBY K-6G) and Reactive Brilliant Red K-2BP (RBR K-2BP) on the activated carbon were evaluated.

2. Materials and methods

2.1. Materials

Corn straw was obtained from the farmland of northern suburb in Taiyuan city of Shanxi province. RBY K-6G (50662-99-2) and RBR K-2BP (70210-20-7) were purchased from Wancai Chemicals and Dyes Department of Shijiazhuang in China.

2.2. Preparation of activated carbon

After washed by clean water, corn straw was dried at 105°C in an oven (HK-351, China). It was then broken to pieces below 20 mesh. The sample was mixed thoroughly with a zinc chloride solution (500 g $ZnCl_2$/100 mL boiled water) according to the mass ratio of 2:1 in a blender. Afterwards, the mixture was put into a 100 mL corundum crucible with a cover (outer diameter of upper opening 60 mm, the outer diameter of lower bottom 36 mm, and height 59 mm) and was irradiated for 6 min at a power level of 700 W in a microwave oven (Midea MM721, China) to obtain the carbide; the carbide was dipped into 3 mol L^{-1} hydrochloric acid solution for half an hour to remove inorganic impurities, filtrated with a vacuum filter (SHB-III, China), washed with deionized water, and then dried to constant weight. The dry particles were ground to pass through 100 mesh sifter, and sealed in plastic bags for further experiments.

2.3. Batch experiments

The adsorption of dosage and initial pH were conducted, adsorption kinetics and thermodynamics were investigated. Firstly, to investigate the effect of dosage, 200 mL of 60 mg L^{-1} dye solution was mixed with 0.05–0.40 g of adsorbent and placed in 2,000 mL Erlenmeyer flask, respectively. These flasks were plugged with parafilm to avoid evaporation and then horizontally shaken with a speed of 120 rpm for 2 h at 25°C in a thermostatic incubator (ZWYH 211D, china). Secondly, to investigate the effect of initial pH, 200 mL of 60 mg L^{-1} dye solution was mixed with 0.2 g of adsorbent in a 2,000 mL Erlenmeyer flask and horizontally shaken for 2 h with the initial pH from 3.0 to 8.0. Thirdly, to investigate adsorption kinetics, 300 mL of 150 mg L^{-1} dye solution was mixed with 0.2 g of adsorbent and shaken for 12 h. The samples were measured by spectrophotometer at intervals between 10 and 720 min. Finally, to investigate adsorption thermodynamics, 50 mL of 120 to 420 mg L^{-1} dye solution was mixed with 0.1 g of adsorbent and shaken for 12 h at 298, 308, and 313 K, respectively. All samples were analyzed by a UV-vis-spectrophotometer (752N, China).

The decolorization rate was obtained by using Eq. (1):

$$\phi = \frac{C_0 - C_1}{C_1} \times 100\% \tag{1}$$

where ϕ (100%) is decolorization rate, C_0 and C_1 (mg L^{-1}) are the dye concentration in solution before and after adsorption, respectively.

The adsorption capacity was obtained by Eq. (2):

$$q_t = \frac{\left(C_0 - C_1\right)V}{m} \tag{2}$$

where q_t (mg g^{-1}) is the adsorption capacity; V (L) is the solution volume; m (g) is the adsorbent weight.

3. Results and discussion

3.1. Characterization of AC

3.1.1. Porous structure of AC

Specific surface area and pore structure were analyzed by ASAP-2020 analyzer (Micromeritics, USA). The S_{BET} of the activated carbon was 937 m^2 g^{-1}, the specific surface of Langmuir was 1,532 m^2 g^{-1}, the total pore volume was 0.7174 cm^3 g^{-1}, the mean pore size was 3.06 nm. The N_2 adsorption–desorption isotherms and the BJH curve are shown in Figs. 1, 2.

According to IUPAC, the N_2 adsorption–desorption isotherms in Fig. 1 was similar to type I adsorption isotherm, and the adsorption isotherm was concave with the P/P_0. When the P/P_0 is greater than 0.8, a horizontal platform is gradually formed, which showed that the adsorption is mainly microporous, and the slope of the platform under high relative pressure is caused by multi-layer adsorption on non-microporous surfaces (such as mesopores or macropores and outer surfaces). The BJH curve in Fig. 2 shows that the pore size distribution is relatively narrow, and the maximum pore radius appears near 1.9 nm, indicating that the pores in the activated carbon are mainly micropores, which is consistent with the result in Fig. 1.

3.1.2. SEM of AC

The appearance of the activated carbon was determined by scanning electron microscope (Hitachi S-4800, Japan), as shown in Fig. 3.

The surface of straw activated carbon is rough and has many small holes, which can effectively remove color and the pollutants.

3.1.3. Functional groups of AC

The adsorption process of activated carbon is not only affected by the pore structure, but also by the surface

chemical properties. Besides carbon atoms, there are H, O, N, S, and other heteroatoms in activated carbon, these heteroatoms usually combine in the edge of the carbon microcrystalline layer, and exist in the form of carboxyl group, lactone group, phenolic hydroxyl group, carbonyl group, and other acidic or alkaline functional groups, which often affect the hydrophilicity of activated carbon, adsorption selectivity, surface pH value, and so on [19]. The functional groups on the carbon surface are determined by Boehm's titration method in this work [20–22], the results were as follows: carboxyl group 1.132 mmol g^{-1}, lactone group 0.916 mmol g^{-1}, phenolic hydroxyl group 0.697 mmol g^{-1}, and total acidity 2.745 mmol g^{-1}.

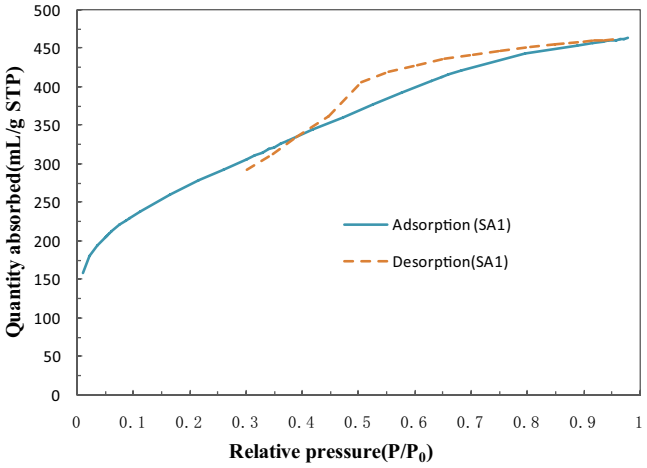

Fig. 1. N_2 adsorption–desorption isotherms.

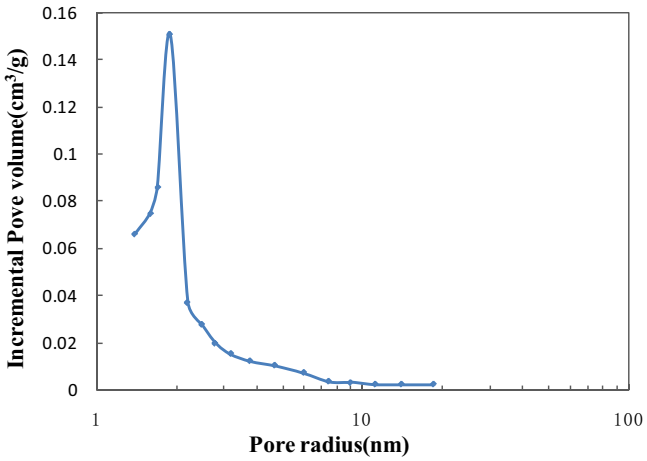

Fig. 2. Curve of BJH.

3.2. Influence of dosage

The influences of the dosage of the activated carbon on the decolorization rate of RBY K-6G and RBR K-2BP are shown in Fig. 4.

Fig. 4 shows that the decolorization rate of RBY K-6G and RBR K-2BP both increased rapidly from the starting point to 1.5 g L^{-1}, then the increase of decolorization rate began to slow down, and the curve became flat. This was because that the vacant adsorption sites increased with the increase of dosage, more dye molecules could be adsorbed onto the activated carbon from liquid phase. However, as adsorption preceded, the dye molecules in solution went on decreasing, the adsorption driving force would be weakened. Therefore, when the dosage was more than 2 g L^{-1}, the change of adsorption capacities was not significant, but the cost of adsorbent would be higher. The decolorization rate of RBY K-6G and RBR K-2BP achieved 79.3% and 83.4% at 2 g L^{-1} of the dosage, respectively.

3.3. Influence of initial pH

Fig. 5 shows the decolorization rate of RBY K-6G and RBR K-2BP at different initial pH.

Fig. 5 shows that the decolorization rate of RBY K-6G and RBR K-2BP increased with the decrease of initial pH. The decolorization rate of RBY K-6G and RBR K-2BP was increased by 18.61% and 9.18% at initial pH 3 when compared with those at initial pH 8, respectively. This possibly because RBY K-6G and RBR K-2BP are anionic dyes, with a large number of anionic groups, such as ($-SO_3^-$). In an acidic environment, electrostatic attraction between the dye molecules and adsorbents are enhanced by the

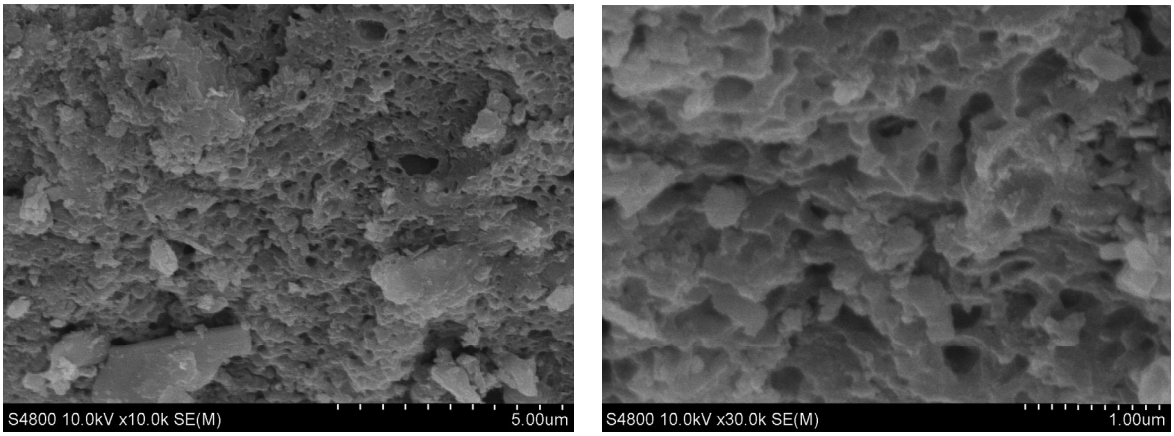

Fig. 3. SEM micrograph of AC.

protonation effect of the functional group (–SO_3^-). As a result, the increase of hydrogen ion concentration was favorable for the adsorptions of RBY K-6G and RBR K-2BP.

3.4. Adsorption kinetics

Pseudo-first-order kinetic model [23]:

$$\ln\left(q_e - q_t\right) = \ln q_e - k_1 t \tag{3}$$

Pseudo-second-order kinetic model [24]:

$$\frac{t}{q_t} = \frac{1}{k_2 q_e^2} + \frac{t}{q_e} \tag{4}$$

Intra-particle diffusion model was proposed by [25]:

$$q_t = k_p t^{0.5} \tag{5}$$

Elovich equation [26,27]:

$$q_t = \frac{1}{\beta}\ln\left(\alpha\beta\right) + \frac{1}{\beta}\ln t \tag{6}$$

where q_e (mg g^{-1}) is the adsorption capacity at equilibrium; k_1 (min^{-1}), k_2 (g mg^{-1} min^{-1}), k_p (mg g^{-1} min$^{-0.5}$)) is the adsorption rate constant for Eqs. (3)–(5), respectively; α (g mg^{-1} min^{-1}) and β (g mg^{-1}) are the adsorption and the desorption constant for Eq. (6).

The experimental data were fitted by using Eqs. (3)–(6). The fitting curve and parameters are shown in Fig. 6 and Table 1.

It can be seen from R^2 in Fig. 6 and Table 1, the pseudo-second-order kinetic model (R^2: 0.9968, 0.9959) had higher fitting degree than intra-particle diffusion equation (R^2: 0.9912, 0.9881), pseudo-first kinetic model (R^2: 0.9602, 0.9200), and Elovich equation (R^2: 0.9520, 0.8860). The Fitting curve of q_t and $t^{0.5}$ did not pass the original point ($C \neq 0$). The equilibrium adsorption capacity of RBY K-6G and RBR K-2BP (95.24, 156.25 mg g^{-1}) were close to the experimental values

Table 1
Parameters of four kinetic models

Model	Dye	Fitting parameters			R^2
		k_1 (min^{-1})	$q_{e,cal}$ (mg g^{-1})	$q_{e,exp}$ (mg g^{-1})	
Pseudo-first-order model	RBY K-6G	0.0072	33.05	96.95	0.9602
	RBR K-2BP	0.0043	61.71	153.36	0.9200
		k_2 (g mg^{-1} min^{-1})	$q_{e,cal}$ (mg g^{-1})	$q_{e,exp}$ (mg g^{-1})	
Pseudo-second-order model	RBY K-6G	0.00082	95.24	96.95	0.9968
	RBR K-2BP	0.00019	156.25	153.36	0.9959
		k_p (g mg^{-1} min$^{0.5}$)			
Intra-particle diffusion equation	RBY K-6G		1.853		0.9912
	RBR K-2BP		2.215		0.9881
		α (g mg^{-1} min^{-1})		β (g mg^{-1})	
Elovich equation	RBY K-6G	18.59		0.1167	0.9520
	RBR K-2BP	9.82		0.0777	0.8860

*$q_{e,cal}$ represents equilibrium adsorption capacity obtained by calculation, *$q_{e,exp}$ represents equilibrium adsorption capacity obtained by experiments.

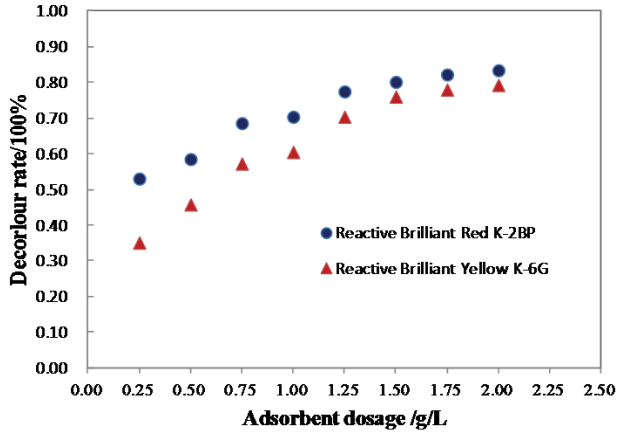

Fig. 4. Influence of the dosage on decolorization rate.

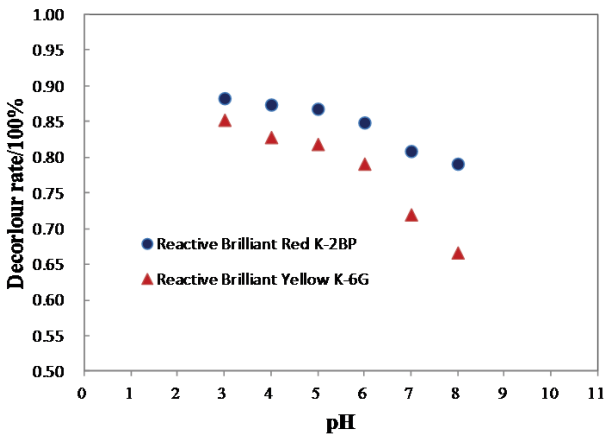

Fig. 5. Influence of the initial pH on decolorization rate.

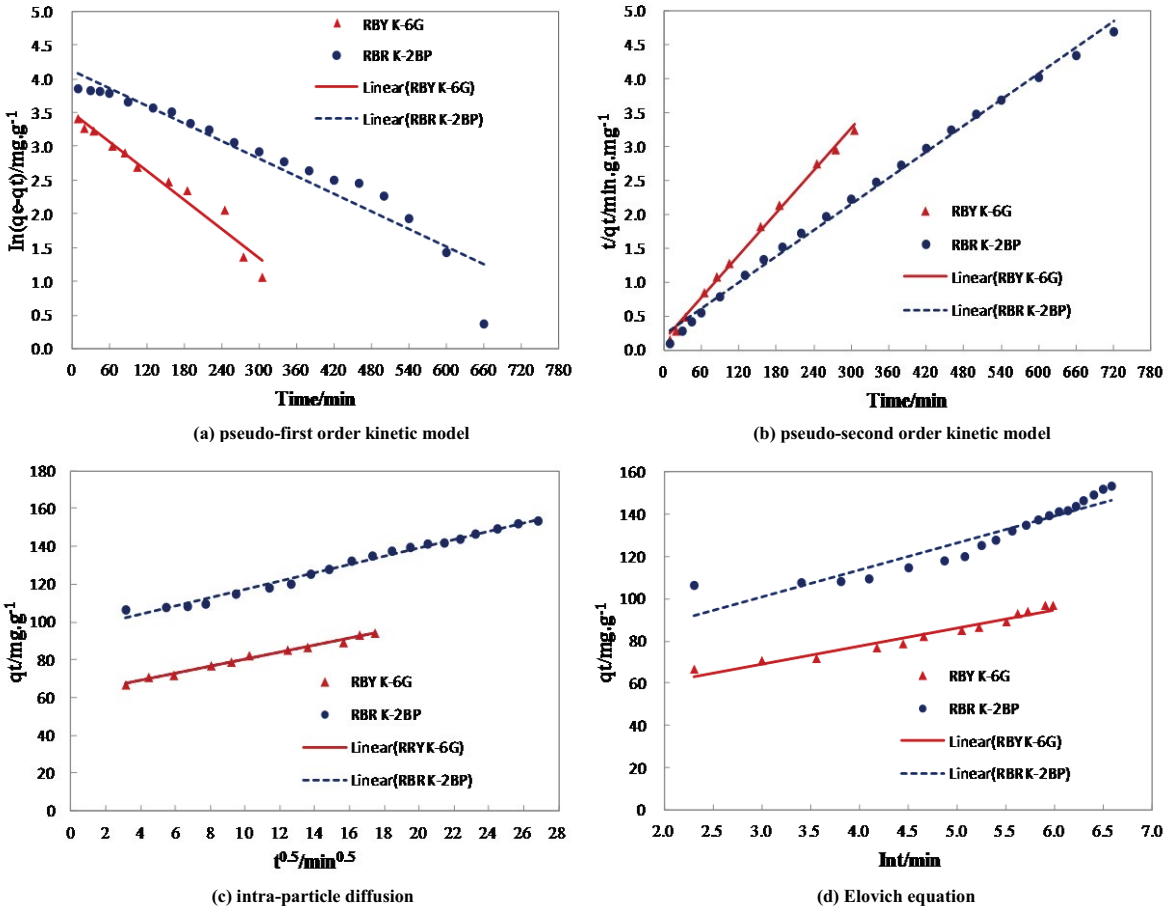

Fig. 6. Fitting curves of four kinetic models. (a) pseudo-first-order kinetic model, (b) pseudo-second-order kinetic model, (c) intra-particle diffusion, and (d) Elovich equation.

(96.95, 153.36 mg g^{-1}), which obtained by pseudo-second-order kinetic model.

As a result, the adsorption of the RBY K-6G and RBR K-2BP conformed to the pseudo-second-order kinetic model. Indicating the higher the number of unoccupied sites, the higher the adsorption rate, which was probably in proportion to the square value of unoccupied sites. The chemical adsorption might be the main mechanism, which involved electronic pair bond sharing or charge transfer between dye molecules and adsorbent. The results were consistent with the literatures [1,14,16].

3.5. Adsorption isotherms

Langmuir model [28]:

$$\frac{c_e}{q_e} = \frac{1}{k_L q_m} + \frac{c_e}{q_m} \tag{7}$$

Freundlich model [29]:

$$\ln q_e = \frac{1}{n}\ln c_e + \ln k_F \tag{8}$$

Temkin equation [30]:

$$q_e = A + B\ln c_e \tag{9}$$

where k_L (L mg^{-1}) and k_F ((mg g^{-1}) (mg $L^{-1})^{-(1/n)}$) are Langmuir and Freundlich constant; n is the surface covering experience constant; A and B are Temkin equation constants.

The fitting curves of the RBY K-6G and RBR K-2BP are shown in Fig. 7, and the parameters of the fitting curves are shown in Table 2.

It can be seen from the R^2 (Table 2) and Fig. 7 that Langmuir fitting curves of RBY K-6G and RBR K-2BP were better (RBY K-6G R^2: 0.9970–0.9996; RBR K-2BP R^2: 0.9832–0.9908) than those of Freundlich model (RBY K-6G R^2: 0.9290–0.9554; RBR K-2BP R^2: 0.9362–0.9760) and Temkin equation (RBY K-6G R^2: 0.9564–0.9727; RBR K-2BP R^2: 0.9244–0.9731). It could be suggested that the surface of the adsorbent from corn straw was uniform, and the adsorption was mainly monolayer [14,31]. The activated carbon had good adsorption performances for RBY K-6G and RBR K-2BP, and the Langmuir maximum adsorption capacities of RBY K-6G and RBR K-2BP were 140.85 and178.57 mg g^{-1} at 318 K, respectively.

3.6. Thermodynamic parameters

$\Delta G°$, $\Delta H°$, and $\Delta S°$ were obtained by Eqs. (10)–(12):

$$\Delta G = RT\ln K \tag{10}$$

$$K_c = \frac{q_e}{c_e} \tag{11}$$

Table 3
Thermodynamic parameters

Dyestuff	$\Delta H°$ (kJ mol^{-1})	$\Delta S°$ (J mol^{-1} K^{-1})	$\Delta G°$ (kJ mol^{-1})		
			298 K	308 K	318 K
RBY K-6G	1.61	29.05	–7.05	–7.34	–7.63
RBR K-2BP	1.41	28.47	–7.08	–7.36	–7.65

Table 2
Fitting parameters of isotherms

Models	Temperature (K)	RBY K-6G			RBR K-2BP		
		k_L (L mg^{-1})	q_m (mg g^{-1})	R^2	k_L (L mg^{-1})	q_m (mg g^{-1})	R^2
Langmuir isotherm	298	0.0851	93.46	0.9970	0.0298	156.25	0.9858
	308	0.0962	126.58	0.9996	0.0604	172.41	0.9908
	318	0.116	140.85	0.9990	0.0779	178.57	0.9832
		k_F (mg g^{-1}) (mg L^{-1})$^{-(1/n)}$	n	R^2	k_F (mg g^{-1}) (mg L^{-1})$^{-1/n}$	n	R^2
Freundlich isotherm	298	34.80	5.27	0.9554	19.83	2.57	0.9760
	308	44.99	4.90	0.9290	39.87	3.42	0.9685
	318	57.67	5.68	0.9441	54.73	4.23	0.9362
		A (mg g^{-1})	B (L g^{-1})	R^2	A (mg g^{-1})	B (L g^{-1})	R^2
Temkin isotherm	298	21.56	13.32	0.9727	-46.25	35.58	0.9731
	308	26.38	19.20	0.9628	-3.67	33.27	0.9723
	318	41.09	19.14	0.9564	20.43	30.42	0.9244

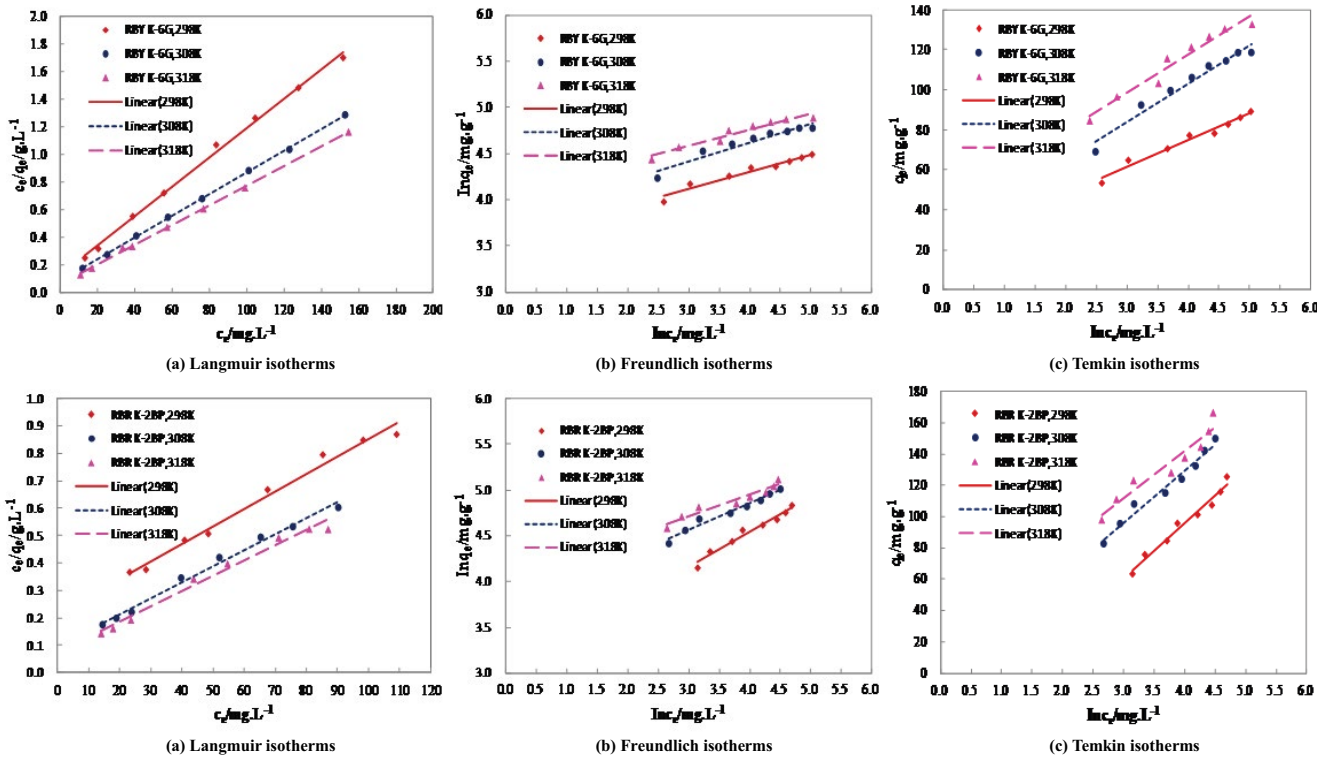

Fig. 7. Adsorption isotherms of RBY K-6G and RBR K-2BP. (a) Langmuir isotherms, (b) Freundlich isotherms, and (c) Temkin isotherms.

Table 4
Comparison of the activated carbons in literatures

Materials	Preparation conditions	Activator	S_{BET} ($m^2\ g^{-1}$)	Reference
Orange peel	Microwave power 700 W for 10 min	KOH	1,015	[33]
Albizia lebbeck seed pods	Microwave power 620 W for 8 min	KOH	1,825	[34]
Peanut shells	Microwave power 700 W for 20 min	H_2SO_4	396	[35]
Oil palm fiber	Microwave power 360 W for 5 min	$ZnCl_2$	708	[36]
Oil palm empty fruit bunch	Microwave power 360 W for 15 min	KOH	808	[37]
Corn straw	800°C for 90 min	$ZnCl_2$	1,056	[38]
Capsicum straw	400°C for 50 min	KOH	966	[39]
Capsicum straw	700°C for 60 min	KOH	676	[40]
Rice straw	600°C for 60 min	H_3PO_4	372	[41]
Wheat straw	700°C for 60 min	$ZnCl_2$	907	[42]
Corn Straw	Microwave power 700 W for 6 min	$ZnCl_2$	937	This work

$$\ln K_c = -\frac{\Delta H}{RT} + \frac{\Delta S}{R} \tag{12}$$

The slope and intercept can be obtained from plots of $\ln K_c$ vs $1/T$. $\Delta H°$, $\Delta S°$, and $\Delta G°$ were calculated by Eqs. (10)–(12), the results are shown in Table 3.

$\Delta H > 0$ illustrated the adsorption was endothermic, and higher temperature was in favor of the adsorption of RBY K-6G and RBR K-2BP. $\Delta S° > 0$ illustrated that the disorder of the whole system increased when dye molecules were adsorbed to the activated carbon from free state in solution. $\Delta G° < 0$ indicated that the adsorption was spontaneous [32].

3.7. Comparison of different activated carbons

Generally speaking, porous materials with large specific surface area have strong adsorption capacity. Standard test method for specific surface area is multipoint Brunauer–Emmett–Teller (BET) nitrogen adsorption, which developed by Bruner, Emmett, and Teller. In order to further illustrate the advantages of the activated carbon prepared in this work, we have consulted many related literature in recent years, and compared their preparation process and BET specific surface area. The results are shown in Table 4.

As we all know, there are many factors which can affect the adsorption capacity of activated carbon, such as raw materials, activators, and preparation process. The S_{BET} of the activated carbon prepared by microwave method can reach 1,825 $m^2\ g^{-1}$ [34], which is highest in Table 4. The S_{BET} of the activated carbon prepared by traditional heating method can reach 1,056 $m^2\ g^{-1}$ [38], which shows the high-performance activated carbon can be obtained by microwave method, but the time is greatly shortened. In the mixing process of raw materials and activators, the dry way is adopted in this work, which is different from the wet way (immersion method) in other literatures. The S_{BET} of the activated carbon prepared in this work reaches 937 $m^2\ g^{-1}$, which is higher than that of the activated carbons in literatures [35,36,37,40,41,42], indicating that the dry way can be an alternative to the wet way. Compared to the wet way, the dry way can simplify the process, and cut down the production cycle, and reduce the energy consumption and the cost.

4. Conclusions

- The activated carbon from corn straw was developed by microwave irradiation, the S_{BET} of the activated carbon achieved 937 $m^2\ g^{-1}$. Compared to traditional heating time of about 60 min above 400°C, the microwave radiation time is only 6 min at 700 W in this paper, which indicating that microwave pyrolysis can save more time than traditional heating pyrolysis. Microwave pyrolysis is a promising method for the reutilization of agricultural wastes.
- The activated carbon is high efficient for remove reactive dyes from aqueous solution. Langmuir maximum adsorption capacities of RBY K-6G and RBR K-2BP were 140.84 and 178.57 mg g^{-1} at 318 K, respectively. The adsorption for two dyes was both comforted to pseudo-second-order kinetic model and Langmuir isotherm.
- Compared with the traditional immersion method for mixing the material and activator, the dry way used in this paper, that is, the material and the active agent are directly mixed under the dry state, is a potential approach.

Acknowledgments

This work was supported by the Natural Science Foundation of Shanxi Province [2015011018], key science foundation of Taiyuan Institute of Technology [2018LG03] and the Fund for Shanxi "1331 project" Collaborative Innovation Center.

References

[1] H. Sohrabi, E. Ameri, Adsorption equilibrium, kinetics, and thermodynamics assessment of the removal of the Reactive Brilliant Red 141 dye using sesame waste, Desal. Water Treat., 57 (2016) 18087–18098.
[2] P. Sakthisharmila, P.N. Palanisamy, P. Manikandan, A characteristic study on generation and interactive effect of electrocoagulated floc with Direct Green 1 and Reactive Brilliant Red 2, J. Mol. Liq., 231 (2017) 160–167.

[3] W.T. Mook, M.K. Aroua, M. Szlachta, C.S. Lee, Optimisation of Reactive Black 5 dye removal by electrocoagulation process using response surface methodology, Water Sci. Technol., 75 (2017) 952–962.
[4] O. Arciniega Cano, C.A. Rodríguez González, J.F. Hernández Paz, P. Amezaga Madrid, P.E. García Casillas, A.L. Martínez Hernández, C.A. Martínez Pérez, Catalytic activity of palladium nanocubes/multiwalled carbon nanotubes structures for methyl orange dye removal, Catal. Today, 282 (2017) 168–173.
[5] Q. Tian, W. Wu, S. Yang, G. Liu, W. Yao, F. Ren, C. Jiang, Zinc oxide coating effect for the dye removal and photocatalytic mechanisms of flower-like MoS_2 nanoparticles, Nanoscale Res. Lett., 12 (2017), doi: 10.1186/s11671-017-2005-0.
[6] E.B. Benidris, M.R. Ghezzar, A. Ma, B. Ouddane, A. Addou, Water purification by a new hybrid plasma-sensitization-coagulation process, Sep. Purif. Technol., 178 (2017) 253–260.
[7] R.A. Pereira, M.F.R. Pereira, M.M. Alves, L. Pereira, Carbon based materials as novel redox mediators for dye wastewater biodegradation, Appl. Catal., B, 144 (2014) 713–720.
[8] S.S. Moghaddam, M.R.A. Moghaddam, Aerobic granular sludge for dye biodegradation in a sequencing batch reactor with anaerobic/aerobic cycles, Clean Soil Air Water, 44 (2016) 438–443.
[9] G. Mezohegyi, F.P. van der Zee, J. Font, A. Fortuny, A. Fabregat, Towards advanced aqueous dye removal processes: a short review on the versatile role of activated carbon, J. Environ. Manage., 102 (2012) 148–164.
[10] I. Koyuncu, Reactive dye removal in dye/salt mixtures by nanofiltration membranes containing vinylsulphone dyes: effects of feed concentration and cross flow velocity, Desalination, 143 (2002) 243–253.
[11] M.T. Yagub, T.K. Sen, S. Afroze, H.M. Ang, Dye and its removal from aqueous solution by adsorption: a review, Adv. Colloid Interface Sci., 209 (2014) 172–184.
[12] M. Qiu, S. Xiong, J. Lin, Adsorption kinetics of dye wastewater in aqueous solution by activated carbon from capsicum straw, Int. J. Environ. Technol. Manage., 19 (2017) 91–102.
[13] J.F. Honório, M.T. Veit, G.C. Gonçalves, É.A. de Campos, M.R. Fagundes-Klen, Adsorption of reactive blue BF-5G dye by soybean hulls: kinetics, equilibrium and influenceing factors, Water Sci. Technol., 73 (2016) 1166–1174.
[14] G.M. Ratnamala, U.B. Deshannavar, S. Munyal, K. Tashildar, S. Patil, A. Shinde, Adsorption of reactive blue dye from aqueous solutions using sawdust as adsorbent: optimization, kinetic, and equilibrium studies, Arabian J. Sci. Eng., 41 (2016) 333–344.
[15] B. Balci, F.E. Erkurt, Adsorption of reactive dye from aqueous solution and synthetic dye bath wastewater by eucalyptus bark/magnetite composite, Water Sci. Technol., 74 (2016) 1386–1397.
[16] S.Q. Hu, Y.H. Chen, K. Xie, X. Qi, T.R. Zhu, Adsorption properties of Reactive Brilliant Red X-3B, Reactive Light Yellow K-6G and Reactive Brilliant Blue X-BR on ethylenediamine-modified magnetic chitosan microspheres, Adv. Mater. Res., 864–867 (2014) 659–663.
[17] P.V. Thitame, S.R. Shukla, Adsorptive removal of reactive dyes from aqueous solution using activated carbon synthesized from waste biomass materials, Int. J. Environ. Sci. Technol., 13 (2016) 561–570.
[18] M.E. Mahmoud, G.M. Nabil, N.M. El-Mallah, H.I. Bassiouny, S. Kumar, T. Abdel-Fattah, Kinetics, isotherm, and thermodynamic studies of the adsorption of Reactive Brilliant Red 195 A dye from water by modified switchgrass biochar adsorbent, J. Ind. Eng. Chem., 37 (2016) 156–167.
[19] N. Wibowo, L. Setyadhi, D. Wibowo, J. Setiawan, S. Ismadji, Adsorption of benzene and toluene from aqueous solutions onto activated carbon and its acid and heat treated forms: influence of surface chemistry on adsorption, J. Hazard. Mater., 146 (2007) 237–242.
[20] A. Pawlicka, B. Doczekalska, Determination of surface oxygen functional groups of active carbons according to the Boehm's titration method, For. Wood Technol., 84 (2013) 11–14.
[21] T.J. Bandosz, Effect of pore structure and surface chemistry of virgin activated carbons on removal of hydrogen sulfide, Carbon, 37 (1999) 483–491.
[22] H.P. Boehm, Some aspects of the surface chemistry of carbon blacks and other carbons, Carbon, 32 (1994) 759–769.
[23] Z. Aksu, Biosorption of reactive dyes by dried activated sludge: equilibrium and kinetic modeling, Biochem. Eng. J., 7 (2001) 79–84.
[24] Y.S. Ho, G. McKay, Pseudo-second-order model for sorption processes, Process Biochem., 34 (1999) 451–465.
[25] W.J. Weber, J.C. Morris, Proceeding of International Conference on Water Pollution Symposium, Pergamon Press, Oxford, UK, 1962.
[26] J. Shou, M. Qiu, Adsorption kinetics of phenol in aqueous solution onto activated carbon from wheat straw lignin, Desal. Water Treat., 57 (2016) 3119–3124.
[27] M.D. Low, Kinetics of chemisorption of gases on solids, Chem. Rev., 60 (1960) 267–312.
[28] I. Langmuir, The constitution and fundamental properties of solids and liquids, J. Am. Chem. Soc., 38 (1916) 2221–2295.
[29] H. Freundlich, W. Heller, The adsorption of cis- and trans-azobenzene, J. Am. Chem. Soc., 61 (1939) 2228–2230.
[30] J.A. Mead, A comparison of the Langmuir, Freundlich and Temkin equations to describe phosphate adsorption properties of soils, Soil Res., 19 (1981) 333–342.
[31] X.L. Ren, L. Yang, M. Liu, Kinetic and thermodynamic studies of acid scarlet 3R adsorption onto low-cost adsorbent developed from sludge and straw, Chin. J. Chem. Eng., 22 (2014) 208–213.
[32] D. Pathania, S. Sharma, P. Singh, Removal of methylene blue by adsorption onto activated carbon developed from *Ficus carica* bast, Arabian J. Chem., 10 (2017) 1445–1451.
[33] S.S. Lam, R.K. Liew, Y.M. Wong, E. Azwar, A. Jusoh, R. Wahi, Activated carbon for catalyst support from microwave pyrolysis of orange peel, Waste Biomass Valorization, 8 (2017) 2109–2119.
[34] M.J. Ahmed, S.K. Theydan, Fluoroquinolones antibiotics adsorption onto microporous activated carbon from lignocellulosic biomass by microwave pyrolysis, J. Taiwan Inst. Chem. Eng., 45 (2014) 219–226.
[35] J. Georgin, G.L. Dotto, M.A. Mazutti, E.L. Foletto, Preparation of activated carbon from peanut shell by conventional pyrolysis and microwave irradiation-pyrolysis to remove organic dyes from aqueous solutions, J. Environ. Chem. Eng., 4 (2016) 266–275.
[36] K.Y. Foo, B.H. Hameed, Microwave-assisted preparation of oil palm fiber activated carbon for methylene blue adsorption, Chem. Eng. J., 166 (2011) 792–795.
[37] K.Y. Foo, B.H. Hameed, Preparation of oil palm (Elaeis) empty fruit bunch activated carbon by microwave-assisted KOH activation for the adsorption of methylene blue, Desalination, 275 (2011) 302–305.
[38] R. Shi, Y. Li, J. Yin, S. Yang, Preparation of activated carbon from corn straw and research of adsorption kinetics, Chin. J. Environ. Eng., 8 (2014) 3428–3432.
[39] H. Li, Y. Liu, N. Wang, Preparation and characterization of activated carbon from capsicum straw under optimum carbonization process, Chin. J. Process Eng., 17 (2017) 1066–1071.
[40] M. Qiu, Y. Xuan, P. Luo, Z. Wang, J. Shou, Adsorption of methylene blue by activated carbon from capsicum straw, Nat. Environ. Pollut. Technol., 14 (2015) 859–864.
[41] T. Samanmulya, P. Deetae, P. Wongpromrat, A study of atrazine adsorption by using the rice straw synthesized adsorbent, MATEC Web Conf., 192 (2018), doi: 10.1051/matecconf/201819203035.
[42] Y. Ma, Comparison of activated carbons prepared from wheat straw via $ZnCl_2$ and KOH activation, Waste Biomass Valorization, 8 (2017) 1–11.